

Quantitative Temporal-Spatial Distribution of Severe Acute Respiratory Syndrome-Associated Coronavirus (SARS-CoV) in Post-Mortem Tissues

Julian W. Tang,¹ Ka-Fai To,² Anthony W.I. Lo,² Joseph J.Y. Sung,³ H.K. Ng,² and Paul K.S. Chan^{1,3*}

¹Department of Microbiology, School of Public Health, Faculty of Medicine, The Chinese University of Hong Kong, Hong Kong Special Administrative Region, Hong Kong SAR, China

²Department of Anatomical and Cellular Pathology, School of Public Health, Faculty of Medicine, The Chinese University of Hong Kong, Hong Kong Special Administrative Region, Hong Kong SAR, China

³Department of Centre for Emerging Infectious Diseases, School of Public Health, Faculty of Medicine, The Chinese University of Hong Kong, Hong Kong Special Administrative Region, Hong Kong SAR, China

Few post-mortem studies have been performed on patients who have died from severe acute respiratory syndrome (SARS). No studies have examined how the SARS-associated coronavirus (SARS-CoV) loads in different organs with respect to time, post-mortem. The aim of this study was to determine the quantitative temporal-spatial distribution of SARS-CoV in the post-mortem tissue samples of seven patients. Quantitation of a house-keeping gene, glyceraldehyde-3-phosphate dehydrogenase (GAPDH) was undertaken to standardize the amount of tissue tested. SARS-CoV viral load and SARS-CoV/GAPDH RNA ratio for each organ type were related to four time durations: onset of illness to death, death to post-mortem tissue sampling, and total durations of treatment with ribavirin and hydrocortisone. The SARS-CoV/GAPDH RNA ratio remained relatively stable in most organ tissue types for all these time durations. The ratio reached the highest value of equal to or greater than one for lung and small bowel, whereas those for heart, liver, spleen, and kidney were always less than one. It is concluded that SARS-CoV viral loads in these organs remain relatively stable, post-mortem. This quantitative assessment further supports SARS-CoV has a specific tropism for the human respiratory and gastrointestinal tracts, which may be related to the density of SARS-CoV receptors. *J. Med. Virol.* 79:1245–1253, 2007. © 2007 Wiley-Liss, Inc.

KEY WORDS: coronavirus; post-mortem; SARS; tropism; viral load; organ

INTRODUCTION

During and after the worldwide severe acute respiratory syndrome (SARS) epidemics of 2003, many studies

concentrated on the characterization of the SARS-associated coronavirus (SARS-CoV) and its receptor. As a starting point, several studies determined the presence of SARS-CoV in different organs. Such studies examined post-mortem tissue directly to determine the pattern of SARS-CoV infection in humans. These studies focused necessarily on the more severe cases of SARS that lead to death, allowing post-mortem examination of lung tissue [Franks et al., 2003; Nicholls et al., 2003; Chow et al., 2004; Mazzulli et al., 2004; Tse et al., 2004], in both lungs and gut [To et al., 2004], the heart [Zhao et al., 2003; Farcas et al., 2005], the kidney [Zhao et al., 2003; Ding et al., 2004; Farcas et al., 2005], the liver [Chau et al., 2004; Ding et al., 2004; Farcas et al., 2005], the spleen [Farcas et al., 2005], and in tissue from multiple organs [Farcas et al., 2005]. It was shown that the lungs [Lang et al., 2003; Zhao et al., 2003; Chau et al., 2004; Ding et al., 2004; Lee et al., 2004; Shi et al., 2005; Xu et al., 2005] and small bowel [Ding et al., 2004; Chan et al., 2005; Farcas et al., 2005; Shi et al., 2005] are likely to be the major, if not the only, sites of SARS-CoV replication [Peiris et al., 2003; Cheng et al., 2004; Xu et al., 2005].

A specific receptor for SARS-CoV was soon discovered, the angiotensin converting enzyme-2 (ACE-2) [Li et al., 2003]. This is the soluble form of a novel homologue of angiotensin-converting enzyme (ACE), ACE-2 [Li et al., 2003; Xiao et al., 2003; Wang et al., 2004]. However, the

Grant sponsor: Research Fund for the Control of Infectious Diseases from the Health, Welfare, and Food Bureau of the Hong Kong Special Administrative Region Government.

*Correspondence to: Paul K.S. Chan, Department of Microbiology, The Chinese University of Hong Kong, 1/F, Clinical Science Building, Prince of Wales Hospital, Shatin, New Territories, Hong Kong SAR, China.
E-mail: paulkschan@cuhk.edu.hk

Accepted 27 February 2007

DOI 10.1002/jmv.20873

Published online in Wiley InterScience
(www.interscience.wiley.com)

presence of this receptor seems not to be the only determinant for organ tropism [Chan et al., 2004a]. Endothelial cells express high levels of ACE-2, but have not been found to be infected with SARS-CoV [Hamming et al., 2004; To and Lo, 2004; Lau and Peiris, 2005], although systemic vasculitis has been reported in the heart, lung, liver, kidney, adrenal glands, and striated muscle interstitia [Ding et al., 2003]. Soon thereafter, a second SARS-CoV receptor or co-receptor candidate was found, and was shown to be a type 2 transmembrane glycoprotein, CD209L, a C-type lectin, also known as L-SIGN, DC-SIGNR, and DC-SIGN2, which is expressed in type 2 alveolar and endothelial cells and has given further support for specific tissue tropisms for SARS-CoV. This glycoprotein has also been shown to bind other viruses, including Ebola, Sindbis and hepatitis C envelope glycoproteins E1 and E2 [Jeffers et al., 2004].

The present study describes the SARS-CoV RNA loads in the post-mortem tissues of various body organs. These data are not only important for defining better the natural history and tropism of SARS-CoV infection, but also for improving the understanding of the basic pathology of the SARS.

METHODS

Post-Mortem Tissue Sampling

Eleven patients who died of SARS were included. All these patients had laboratory evidence of SARS-CoV infection. Post-mortem tissues were collected with great care from the major organs including heart, kidney, liver, spleen, lung, small bowel, psoas (skeletal) muscle, and bone marrow. To avoid cross-contamination, a new set of forceps and cutting knife was used for each specimen. Each freshly collected tissue lump was cut into two, one for virus isolation and the other stored in -70°C with RNA preservative (RNALater, Qiagen, Hilden, Germany) for later use.

Viral and Host RNA Quantitation

Extraction of viral RNA from tissue. The frozen tissue samples were allowed to thaw on ice. A piece of the tissue measuring around 3 mm^3 was used for RNA extraction. The samples were disrupted using a pestle and mortar. Total RNA was extracted from the tissue samples using a commercial kit according to the manufacturer's instructions (RNeasy Mini Kit, Qiagen). The sample was first grounded in $600\text{ }\mu\text{l}$ of Buffer RLT into a homogeneous lysate, which was then transferred onto a QIAshredder spin column (Qiagen) and centrifuged at $13,000\text{ rpm}$ for 3 min. As grinding only disrupts the cells, final homogenization was achieved by centrifugation through the QIAshredder spin column. Only the supernatant was used for the subsequent steps. Next, $600\text{ }\mu\text{l}$ of 70% ethanol was added to the tissue lysate, mixed by pipetting. The mixture was added to an RNeasy spin column and centrifuged for 15 sec at $13,000\text{ rpm}$. The flow through was discarded. The spin column

was washed once with $700\text{ }\mu\text{l}$ Buffer RW1, then twice with $500\text{ }\mu\text{l}$ Buffer RPE. Viral RNA was eluted in $50\text{ }\mu\text{l}$ of RNAase-free water.

Qualitative SARS-CoV RT-PCR screening assay.

The extracted nucleic acid from each of the post-mortem tissue specimens was initially screened for SARS-CoV using an in-house qualitative reverse transcription polymerase chain reaction (RT-PCR) assay described previously [Chan et al., 2004b], as well as by virus isolation. Only those specimens positive by the RT-PCR assay were then used for the quantitative SARS-CoV real-time PCR assay (Table I). In some cases SARS-CoV was detected by the initial qualitative assay, but the remaining amount of specimen was insufficient for the subsequent quantitative assay.

SARS-CoV isolation. For SARS-CoV isolation, specimens were minced and inoculated onto African green monkey (Vero E6) cell monolayers. The subsequent growth, detection and identification of SARS-CoV were performed under Biosafety Containment Level 3 facilities, as described previously [Chan et al., 2004b].

SARS-CoV real-time RT-PCR assay. A real-time RT-PCR kit was used for the quantitation of SARS-CoV RNA, according to the manufacturer's protocol (Aplimedical spa, Bioline, Italy). Briefly, $10\text{ }\mu\text{l}$ of the RNA extract was reversely transcribed to cDNA with random hexamers in a reaction volume of $25\text{ }\mu\text{l}$. Five microliters of cDNA was added to a final reaction volume of $25\text{ }\mu\text{l}$ for quantitative real-time PCR. Standards containing 1×10^2 to 1×10^5 copies of TOR2 plasmid per $5\text{ }\mu\text{l}$ were used for calibration. The reactions were performed using Q-SARS coronavirus AmpliMASTER, Q-SARS coronavirus AmpliMIX and Q-SARS coronavirus AmpliPROBE, which contains the reagent mix, primers and probe, respectively. The thermal cycling conditions were: 50°C for 2 min, 95°C for 10 min, followed by 45 cycles of: 95°C for 15 sec and 60°C for 1 min. Samples and standards were tested in duplicate.

GAPDH real-time RT-PCR assay. To standardize the amount of host tissue examined in each tissue sample, the RNA transcript of a housekeeping gene, glyceraldehyde-3-phosphate dehydrogenase (GAPDH) was quantified using a real-time PCR kit (GAPDH RNA control kit, Applied Biosystems, Foster City, CA). Briefly, $1\text{ }\mu\text{l}$ of extracted RNA was used as the template in a reaction volume of $25\text{ }\mu\text{l}$. All of the cDNA produced in this RT reaction was used in the subsequent quantitative PCR. Standards containing known copies of GAPDH were also included in the assay. Samples and standards were tested in duplicate. Negative controls were included to detect any cross-contamination. The thermal cycling conditions were: 50°C for 2 min, 60°C for 30 min, 95°C for 5 min followed by 40 cycles of 95°C for 15 sec and 62°C for 1 min.

The SARS-CoV and GAPDH RNA loads/ 3 mm^3 tissue extract, were expressed separately, and also as a SARS-CoV/GAPDH RNA ratio. This method of expressing these quantitative results was important to obtain a more accurate indication of SARS-CoV RNA concentration in the samples taken from each organ type, as

TABLE I. Qualitative RT-PCR and Virus Isolation Results of Study Patients

Patient	SARS-CoV detection results									
	Heart (RT-PCR/ ISO)	Kidney (RT-PCR/ISO)	Liver (RT-PCR/ISO)	Spleen (RT-PCR/ISO)	Left lung (RT-PCR/ISO)	Right lung (RT-PCR/ISO)	Small bowel (RT-PCR/ISO)	Muscle (RT-PCR/ISO)	Bone marrow (RT-PCR/ISO)	
1	POS/neg	POS/neg	POS/neg	POS/neg	POS/POS	POS/POS	POS/POS	POS/neg	neg/neg	
2	POS/neg	POS/neg	POS/neg	POS/neg	POS/neg	POS/neg	POS/neg	POS/neg		
3	POS/neg	POS/neg	POS/neg	POS/neg	POS/POS	POS/POS	POS/POS	POS/neg		
4	POS/neg	POS/neg	POS/neg	POS/neg	POS/POS	POS/POS	POS/POS	POS/neg		
5	POS/neg	POS/neg	neg/neg	POS/neg	POS/neg	neg/neg	POS/POS	POS/neg		
6	POS/neg	POS/neg	POS/neg	POS/neg	POS/POS	POS/POS	POS/POS	POS/POS		
7	neg/neg	POS/neg	POS/neg	POS/neg	POS/POS	POS/POS	POS/POS	POS/POS		
8	neg/neg	neg/neg	neg/neg	neg/neg	neg/neg	POS/neg	neg/neg	neg/neg	neg/neg	
9	neg/neg	neg/neg	neg/neg	neg/neg	POS/neg	POS/neg	POS/neg	POS/neg		
10	neg/neg	neg/neg	neg/neg	neg/neg	POS/neg	POS/neg	POS/neg	POS/neg		
11	neg/neg	neg/neg	neg/neg	neg/neg	POS/neg	POS/neg	POS/neg	POS/neg		

POS, positive testing result; neg, negative testing result; RT-PCR, qualitative reverse-transcription polymerase chain reaction; ISO, virus isolation by Vero E6 cells; Blank space—tissue not available.

the exact amount and homogeneity of this tissue used in the RNA extraction, could not be characterized precisely.

RESULTS

The age of the 11 studied patients ranged from 44 to 91 years, seven of them were males. None of the patients were healthcare workers. All 11 patients had SARS-CoV detected from one or more organs (Table I). Further quantitative viral load analyses were performed for Patients 1–7, as specimens from Patients 8–11 were not sufficient for these analyses. The details of Patients 1–7 are shown in Table II. They all had pre-morbid disease. Six patients had SARS-CoV isolated from postmortem tissue samples by standard cell culture techniques. Eight of the 12 isolation-positive samples were from lung and the remaining four were from intestine (Table II).

Organ-Specific Viral Loads Related to Duration ('Onset-Death Interval') of SARS Illness

Most of the tissues had detectable SARS-CoV RNA by RT-PCR (Table II). Figures 1–6 show the results, using semi-log plots, for each organ: heart, kidney, liver, spleen, lung, and small bowel, respectively, for SARS-CoV, GAPDH and the SARS-CoV/GAPDH RNA ratio. Each data point in each graph represents a different patient. Since each of these patients survived for a different duration after becoming infected with SARS-CoV, the graphs demonstrate the SARS-CoV RNA loads in these seven different patients, according to their duration of SARS illness. For Patients 2 and 3, SARS-CoV RNA was also detected in the psoas muscle tissue.

Figures 1–6 show how the SARS-CoV loads changed in individual body organs in relation to the duration of SARS illness, that is, the interval between illness onset and time of death. To summarize, in the heart and liver there was a slight peak and plateau in the SARS-CoV/GAPDH RNA ratio around 10–15 days after onset of illness. In the kidney, spleen, and small bowel, the ratio fluctuated around a relatively constant level. For the lung, the ratio fell noticeably from 2 log₁₀ to –2 log₁₀ after 15 days of illness.

Heart. In the heart (Fig. 1), the SARS-CoV RNA loads ranged between 10² and 10⁵ copies/3 mm³ across the x-axis parameters. The GAPDH RNA load also remained fairly stable across all x-axis parameters, with a range of 10⁶–10⁸ copies/3 mm³, giving a SARS-CoV/GAPDH RNA ratio in the range 10^{–5}–10^{–3}. There were no SARS-CoV culture-positive results from any of the heart biopsies taken (Table II). The mean SARS-CoV RNA load was 5.1 × 10³ (SD: 6.8 × 10³) copies/3 mm³, the mean GAPDH RNA load was 1.0 × 10⁷ (SD: 1.5 × 10⁷) copies/3 mm³, and the mean SARS-CoV/GAPDH RNA ratio was 6.5 × 10^{–4} (SD: 8.0 × 10^{–4}).

Kidney. In the kidney (Fig. 2), the SARS-CoV RNA loads ranged between 10² and 10⁴ copies/3 mm³ across the x-axis parameters. The GAPDH RNA load again remained fairly stable across all x-axis parameters, with

TABLE II. Virological Results of Study Samples

Patient no. underlying illness	Sex	Age (years)	Date admitted	Date fever/illness onset	Ribavirin therapy (total, days)	Hydro-cortisone therapy (total, days)	Date/time of death	Onset-death interval (days)	Date/time of sampling	Death-sampling interval (hours)	Specimen type	SARS-CoV isolation	SARS-CoV RNA cop/3cub.mm tissue	SARS-CoV RNA copy/g tissue	GAPDH RNA cop/3cub.mm tissue	SARS-CoV/GAPDH RNA ratio
1 CRHD	M	69	20/2/3	13/3/3	1	0	18/3/3,20:30	5	25/3/3,11:00	160	Kidney ^a Left lung Liver Right lung Small bowel Spleen Heart	neg POS neg POS POS neg neg	3.25E+02 1.01E+08 5.75E+02 4.68E+08 7.85E+06 4.63E+03 5.43E+02	1.08E+05 3.38E+10 1.92E+05 1.56E+11 2.62E+09 1.54E+06 1.81E+05	1.21E+05 1.25E+06 2.81E+06 2.92E+06 9.62E+05 3.32E+05 2.71E+06	2.68E-03 8.12E+01 2.05E-04 1.60E+02 8.17E+00 1.39E-02 2.00E-04
2 Cirrh	M	44	5/3/3	8/3/3	12	10	24/3/3,00:15	16	31/3/3,11:00	155	Left kidney Left lung Liver Psoas muscle Right lung Small bowel Spleen	neg neg neg neg neg neg neg	6.76E+03 8.01E+04 4.58E+02 5.67E+02 5.83E+04 1.85E+08 2.50E+02	2.25E+06 2.67E+07 1.53E+05 7.15E+06 1.94E+07 4.14E+06 8.33E+04	2.23E+05 3.80E-02 1.57E+06 7.15E+06 2.94E+06 4.14E+06 8.50E+05	3.03E-02 3.80E-02 2.91E-04 7.94E-05 1.99E-02 4.47E+01 2.94E-04
3 CRHD	M	79	5/3/3	17/3/3	14	15	30/3/3,16:05	13	4/4/3,11:00	115	Bone marrow Heart Small bowel Kidney ^a Left lung Liver Psoas muscle Right lung Spleen	neg neg POS neg neg neg neg neg neg	1.49E+04 2.58E+08 1.96E+03 7.60E+05 5.60E+04 7.75E+04 5.95E+03 7.72E+03	4.96E+06 8.58E+10 6.53E+05 2.53E+08 1.87E+07 2.58E+07 1.98E+06 2.57E+06	3.23E+07 1.56E+07 1.07E+06 1.16E+06 3.54E+06 1.08E+07 3.36E+05 1.79E+06	4.60E-04 1.66E+01 1.83E-03 6.56E-01 1.58E-02 7.17E-03 1.77E-02 4.32E-03
4 Hyp	F	91	22/4/3	22/4/3	0	0	23/4/3,4:27	1	30/4/3,11:00	175	Left lung Right lung Spleen Right lung Heart	POS neg neg POS neg	4.33E+06 2.88E+08 4.58E+03 8.89E+03	1.44E+09 9.60E+10 1.53E+06 2.96E+06	7.48E+05 1.99E+06 2.30E+06 1.96E+06	5.79E+00 1.45E+02 1.83E-03 4.55E-03
5 MDS	M	76	13/3/3	10/3/3	7	7	21/3/3,21:22	11	28/3/3,11:00	158	Left kidney Left lung Liver Right lung Small bowel Spleen Heart Left lung Right lung	neg neg neg neg neg neg neg neg neg	POS on screening RT-PCR but insufficient for quantitation neg on screening RT-PCR neg on screening RT-PCR 3.46E+08 1.11E+03 4.13E+02 1.48E+03 2.38E+04 1.45E+08 3.14E+07 9.00E+02	neg on screening RT-PCR neg on screening RT-PCR 1.15E+11 3.69E+05 1.38E+05 4.92E+05 5.12E+10 4.83E+10 1.05E+10 3.00E+05	neg on screening RT-PCR neg on screening RT-PCR 9.36E+05 1.69E+05 3.37E+06 5.09E+05 2.31E+06 1.69E+07 1.35E+06 2.24E+06 1.15E+06	3.70E+02 6.54E-03 1.22E-04 2.90E-03 6.66E+01 1.41E-03 1.07E+02 1.40E+01 7.84E-04
7 Hyp	M	81	16/3/3	14/3/3	14	16	4/4/3,16:45	22	8/4/3,11:00	90	Spleen Heart Left lung Right lung	neg neg POS POS	2.15E+04 3.57E+02	7.16E+06 1.19E+05	1.03E+06 6.10E+05	2.08E-02 5.85E-04

Only Patients 1-7 who were included in quantitative viral load analyses are shown in this table. cub mm, mm³, CRHD, chronic renal failure on haemodialysis; Cirrh, cirrhosis, Hyp, hypertension; MDS, myelodysplastic syndrome. ^aLeft or right kidney not specified.

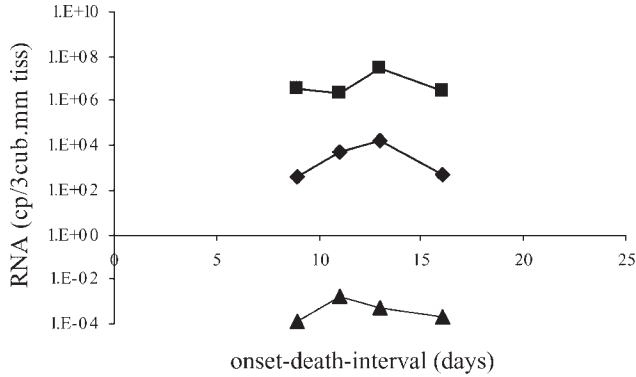


Fig. 1. Heart SARS-CoV RNA (diamonds) and GAPDH RNA (squares) loads and SARS-CoV/GAPDH RNA ratio (triangles) related to each patient's duration of SARS illness (i.e., the 'onset-death interval'). Each data point is from a different patient. In only four patients could the SARS-CoV be quantitated in their heart biopsy samples (see Table II).

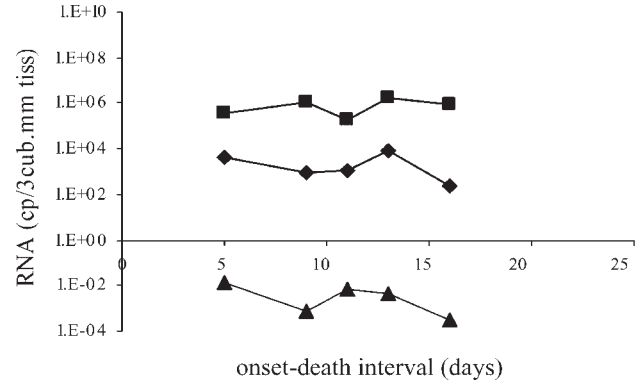


Fig. 4. Spleen SARS-CoV RNA (diamonds) and GAPDH RNA (squares) loads and SARS-CoV/GAPDH RNA ratio (triangles) related to each patient's duration of SARS illness (i.e., the 'onset-death interval'). Each data point is from a different patient. In only five patients could the SARS-CoV be quantitated in their spleen biopsy samples (see Table II).

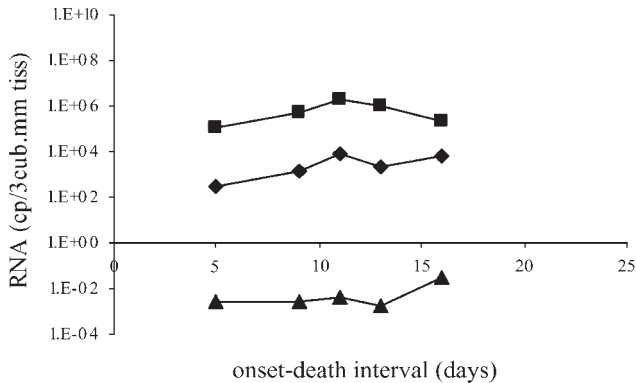


Fig. 2. Kidney SARS-CoV RNA (diamonds) and GAPDH RNA (squares) loads and SARS-CoV/GAPDH RNA ratio (triangles) related to each patient's duration of SARS illness (i.e., the 'onset-death interval'). Each data point is from a different patient. In only five patients could the SARS-CoV be quantitated in their kidney biopsy samples (see Table II). Only one kidney was sampled in each patient.

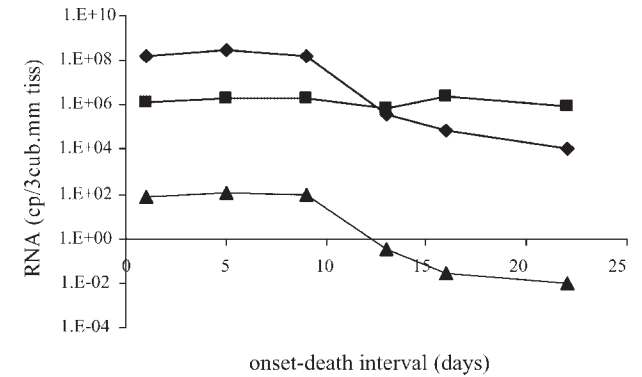


Fig. 5. Lung SARS-CoV RNA (diamonds) and GAPDH RNA (squares) loads and SARS-CoV/GAPDH RNA ratio (triangles) related to each patient's duration of SARS illness (i.e., the 'onset-death interval'). Each data point is from a different patient and represents the mean of the right and left lung SARS-CoV loads. In only five patients could the SARS-CoV be quantitated in their lung biopsy samples (see Table II).

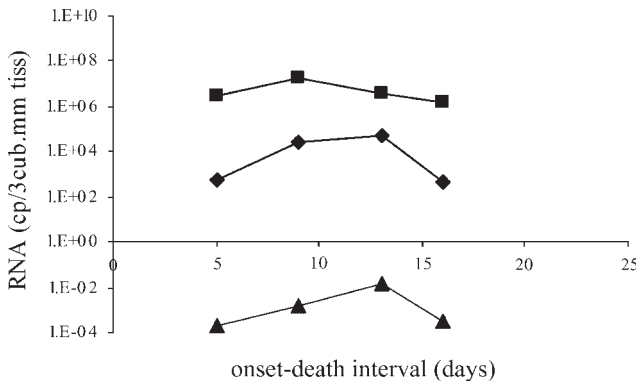


Fig. 3. Liver SARS-CoV RNA (diamonds) and GAPDH RNA (squares) loads and SARS-CoV/GAPDH RNA ratio (triangles) related to each patient's duration of SARS illness (i.e., the 'onset-death interval'). Each data point is from a different patient. In only four patients could the SARS-CoV be quantitated in their liver biopsy samples (see Table II).

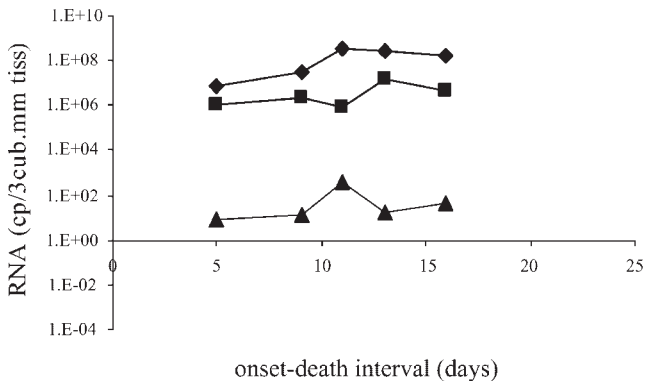


Fig. 6. Small bowel SARS-CoV RNA (diamonds) and GAPDH RNA (squares) loads and SARS-CoV/GAPDH RNA ratio (triangles) related to each patient's duration of SARS illness (i.e., the 'onset-death interval'). Each data point is from a different patient. In only five patients could the SARS-CoV be quantitated in their small bowel biopsy samples (see Table II).

a range of 10^5 – 10^7 copies/3 mm³, giving a SARS-CoV/GAPDH RNA ratio in the range 10^{-3} – 10^{-1} . There were no SARS-CoV culture-positive results from any of the kidney biopsies taken (Table II). The mean SARS-CoV RNA load was 3.9×10^3 (SD: 3.7×10^3) copies/3 mm³. The mean GAPDH RNA load was 7.8×10^5 (SD: 7.6×10^5) copies/3 mm³, and the mean SARS-CoV/GAPDH RNA ratio was 8.4×10^{-3} (SD: 1.2×10^{-2}).

Liver. In the liver (Fig. 3), the SARS-CoV RNA loads were similar to that of heart, ranging 10^2 – 10^5 copies/3 mm³ across the x-axis parameters. The GAPDH RNA load remained fairly stable across all x-axis parameters, with a range of 10^6 – 10^8 copies/3 mm³, giving a SARS-CoV/GAPDH RNA ratio in the range 10^{-4} – 10^{-1} . None of the liver tissue samples examined were positive for SARS-CoV by cell culture (Table II). The mean SARS-CoV RNA load was 2.0×10^4 (SD: 2.6×10^4) copies/3 mm³, the mean GAPDH RNA load was 6.2×10^6 (SD: 7.2×10^6) copies/3 mm³, and the mean SARS-CoV/GAPDH RNA ratio was 4.4×10^{-3} (SD: 7.6×10^{-3}).

Spleen. In the spleen (Fig. 4), the SARS-CoV RNA load was similar to that in the kidney, ranging between 10^2 and 10^4 copies/3 mm³ across all x-axis parameters. The GAPDH RNA load remained fairly stable across all x-axis parameters, with a range of 10^5 – 10^7 copies/3 mm³, giving a SARS-CoV/GAPDH RNA ratio in the range 10^{-4} – 10^{-1} . None of the spleen tissues examined were positive by virus isolation (Table II). The mean SARS-CoV RNA load was 2.9×10^3 (SD: 3.2×10^3) copies/3 mm³. The mean GAPDH RNA load was 8.6×10^5 (SD: 6.5×10^5) copies/3 mm³, and the mean SARS-CoV/GAPDH RNA ratio was 5.2×10^{-3} (SD: 5.5×10^{-3}).

Lung. A mean value was plotted for the SARS-CoV RNA loads in the left and right lungs in Figure 5. The mean lung SARS-CoV RNA load spanned a wider range than all the other organ tissues ranging between 10^4 and 10^9 copies/3 mm³ across the x-axis parameters. The mean GAPDH RNA load for the left and right lungs remained fairly stable across the x-axis parameters, with a more narrow range of 10^5 – 10^7 copies/3 mm³. It can be seen from Figure 5 that the SARS-CoV RNA load exceeded that of GAPDH in the first half, then falls below the GAPDH RNA load in the second half of illness. Thus, the SARS-CoV/GAPDH RNA ratio covered a wide range of 10^{-2} – 10^2 . Eight out of the 14 lung tissue samples taken were SARS-CoV culture positive (from Patients 1, 4, 6, and 7; Table II). The mean SARS-CoV RNA load was 9.7×10^7 (SD: 1.5×10^8) copies/3 mm³, the mean GAPDH RNA load was 1.6×10^6 (SD: 8.8×10^5) copies/3 mm³, and the mean SARS-CoV/GAPDH RNA ratio is 4.7×10^1 (SD: 6.2×10^1).

Small bowel. Small bowel samples showed the highest average organ-specific SARS-CoV RNA load with 10^6 – 10^9 copies/3 mm³ across the x-axis parameters (Fig. 6). The GAPDH RNA load also remained fairly stable across the x-axis parameters, with a range of 10^5 – 10^8 copies/3 mm³, giving a SARS-CoV/GAPDH RNA ratio in the range 10^1 – 10^3 . Four out of the five small bowel tissue samples examined were SARS-CoV cul-

ture-positive (from Patients 1, 3, 5, and 6) (Table II). The mean SARS-CoV RNA load was 1.7×10^8 (SD: 1.5×10^8) copies/3 mm³. The mean GAPDH RNA load was 4.8×10^6 (SD: 6.2×10^6) copies/3 mm³, and the mean SARS-CoV/GAPDH RNA ratio was 9.0×10^1 (SD: 1.6×10^2).

Psoas muscle and bone marrow. Only two patients had psoas muscle and one patient had bone marrow tissue available for this study. Both psoas muscle samples were positive for SARS-CoV at 10^2 – 10^5 copies/3 mm³, with a GAPDH RNA load of 10^6 – 10^8 copies/3 mm³ giving a SARS-CoV/GAPDH RNA ratio in the range 10^{-5} – 10^{-2} . SARS-CoV was not isolated from cell culture of either muscle sample. There was no SARS-CoV detected in the single bone marrow sample, by the qualitative in-house screening RT-PCR or by cell culture (Table II).

Time-Specific Viral Loads

Comparing the SARS-CoV/GAPDH RNA ratios across the different organs, with specific time intervals or durations (see Table II) gives an indication of how SARS-CoV behaves in different organs over time. Although the number of samples was small, some trends were observed.

Death-sampling interval (hours). Table II shows how the SARS-CoV RNA loads changed in individual body organs in relation to the interval between time of death and time of post-mortem sampling. The SARS-CoV and GAPDH RNA levels remain fairly constant up to 180 hr in all the organs except the liver. Only in the liver was there a noticeable drop in SARS-CoV/GAPDH RNA ratio with time, post-mortem, i.e. after about 150 hr, the RNA loads drop by 1–2 log₁₀.

Ribavirin therapy duration (days) and hydrocortisone therapy duration (days). From Table II, it can be seen that ribavirin and hydrocortisone were effectively given in combination for all seven patients, and it is difficult to analyze the RNA loads and ratios with respect to each individual agent. In all organs except the lung, the SARS-CoV RNA load remained fairly constant compared to the GAPDH RNA load, which was reflected in the relatively stable SARS-CoV/GAPDH RNA ratio. In the lung, there was a noticeable drop of about 3–4 log₁₀ in the SARS-CoV/GAPDH RNA ratio, after about days 12–13 of illness.

DISCUSSION

This study examined the presence of viable SARS-CoV and SARS-CoV RNA in post-mortem tissues from 11 patients who died from SARS. In seven patients, sufficient specimens were available for further quantitative viral load analyses. A host cell house-keeping gene (GAPDH) was used to standardize for the amount of tissue obtained from each sample. In the organ-specific viral load results, the overall picture made up from the data points from the seven different patients with different durations of SARS illness, generally, the

SARS-CoV/GAPDH RNA ratio never reached above one in heart, kidney, liver, and spleen tissue for all x-axis parameters analyzed. For the lungs, the initial SARS-CoV/GAPDH RNA ratio was equal to or greater than one, than fell to less than one during the course of illness. For the small bowel, this ratio never fell below one. This ratio can be interpreted as the concentration of SARS-CoV infection in that organ, and may be a good indication of the degree of SARS-CoV tropism, which may in turn reflect the density of the SARS-CoV receptors and co-receptors present in that tissue type.

The range of duration of SARS illness before death (i.e., the 'onset-death interval') for the seven patients studied here, covered the first 3 weeks of illness, ranging from days 5 to 22 post-onset of fever. The SARS-CoV RNA loads in most organs remained relatively stable, despite the samples being taken from different patients at different times after onset of illness. Only in the lung tissue was there a noticeable drop in SARS-CoV RNA load after 12–13 days post-onset of illness. The reason for this is unclear as the SARS-CoV RNA loads in the lungs during ribavirin and hydrocortisone treatment did not reflect this drop at this time. Generally, therefore, there seems to be no change in SARS-CoV RNA levels in these organs from week-to-week during clinical SARS illness. This is in contrast to positive rates or viral loads of SARS-CoV shed in body fluids secreted or excreted from some of these organs systems reported previously [Peiris et al., 2003; Cheng et al., 2004; Hung et al., 2004; Woo et al., 2005]. However, these results on body fluids were made on patients with a wide range of outcome, whereas the current study was on patients with fatal infection where the SARS-CoV viral load could be much higher throughout all body organs at the time of death.

Additional data from Table II on the relationship between the SARS-CoV RNA load with the death-sampling interval, gives some idea of the SARS-CoV viability and the degree of deterioration of the SARS-CoV RNA genome with time, post-mortem. Except for the liver, all organ types exhibited a fairly similar SARS-CoV RNA load, despite being taken from seven different patients, between 90 and 180 hr, post-mortem. As there were no samples taken earlier than 90 hr post-mortem, one could argue that in most of the organs, any deterioration in SARS-CoV and GAPDH RNA levels may have already occurred and reached a nadir by 90 hr post-mortem. In the liver, this deterioration in RNA levels seems to continue after about 150 hr. However, this hypothesis is not supported by the similar ante-mortem levels of SARS-CoV and GAPDH RNA in the onset-death and ribavirin/hydrocortisone treatment data. Taken together, the data suggest that there is actually little fall in RNA levels in these organs, at least up to 180 hr, post-mortem. This implies that SARS-CoV RNA remains detectable in the body tissue of SARS patients for a long period after death, though infectious SARS-CoV was only cultured from the lung and bowel tissue (Table II). The presence of viable SARS-CoV in the lung and bowel biopsies may be due to an overall

viral load effect in that, in these tissues, the considerably higher viral load allowed some viable virus to remain, despite the majority of SARS-CoV possibly losing their viability after the patient's death.

Also noticeable from Table II, apart from the lung, other organs showed little effect of the ribavirin/ hydrocortisone therapy on their SARS-CoV RNA load. The lung SARS-CoV RNA load did fall noticeably after about 12–13 days post-onset of illness, and remained at this lower value during the subsequent continuation of ribavirin and/ or steroid therapy (from 12 to 16 days). Another report on SARS patients' post-mortem lung tissue did not report any significant changes in SARS-CoV viral loads in response to ribavirin and/or corticosteroid use [Mazzulli et al., 2004]. Interestingly, another report showed that early steroid use increases SARS-CoV loads in plasma [Lee et al., 2004], again suggesting that SARS-CoV loads may vary in different ways according to the clinical specimen type tested.

There are limitations to this study. Firstly, the number of patients examined is small. Secondly, it is difficult to accurately quantify the amount of post-mortem tissue taken as the input for the quantitative RNA assay. Although the tissue is described as approximately 3 mm³, as it is not a rigid body, this is necessarily an estimate. Nevertheless, by combining the results from the seven different patients into what may be thought of as a single 'composite' patient, the present study not only quantifies the SARS-CoV spatially within the body's major organs, but also temporally throughout the course of these patients' illness from fever onset to death and post-mortem examination.

Mazzulli et al. [2004] analyzed post-mortem lung tissue using a real-time quantitative SARS-CoV RT-PCR assay, giving levels of 2.7×10^4 – 3.8×10^9 SARS-CoV copies/g tissue. Farcas et al. [2005] used a similar methodology and reported SARS-CoV RNA levels for multiple organs. Table III shows an approximate comparison of the results of the current study and that of Farcas et al. [2005]. It can be seen that the maximum SARS-CoV RNA loads are within one order of magnitude in both studies for the lung, spleen, liver, heart, and kidney. The small bowel and muscle values differ by about two orders of magnitude, but as the number of samples in both studies are relatively low, there may be sampling bias effects (as the SARS-CoV RNA may not be uniformly distributed within an organ), so this difference may not be significant. Using the same comparison criteria, the median SARS-CoV RNA loads for the two studies are also similar for the spleen, heart and kidney, but show more variation for the lung, small bowel, liver, and muscle. Thus, despite these limitations, it can be seen from Table III that the results presented from this study are largely in line with those of Mazzulli et al. [2004] and Farcas et al. [2005].

Angiotensin converting enzyme (ACE) is present in the vascular endothelium of the heart and kidney, and converts another enzyme, angiotensin 1 to its active form, angiotensin 2, which plays a key role in the controlling blood pressure by interacting with the

TABLE III. Comparison of Organ-Specific SARS-CoV RNA Loads Obtained in This Study With Those Reported by Farcas et al. [2005]

Organ	Max SARS-CoV load (copy/g tissue)		Median SARS-CoV load (copy/g tissue)		Patients with SARS-CoV detected in organ % (no./total)	
	Farcas et al.	This study	Farcas et al.	This study	Farcas et al.	This study ^a
Lung	1.0E + 10	1.6E + 11	3.6E + 05	8.5E + 08	100 (19/19)	100 (11/11)
Small bowel	2.7E + 09	1.2E + 11	2.7E + 05	6.2E + 10	73 (11/15)	83 (5/6)
Spleen	7.2E + 05	2.6E + 06	4.8E + 04	3.7E + 05	53 (9/17)	71 (5/7)
Liver	1.6E + 06	1.9E + 07	1.8E + 04	4.1E + 06	41 (7/17)	67 (4/6)
Heart	2.8E + 07	5.0E + 06	3.2E + 04	8.5E + 05	40 (7/18)	50 (4/8)
Kidney	7.4E + 05	3.0E + 06	4.3E + 04	6.5E + 05	38 (6/16)	83 (5/6)
Muscle	2.8E + 04	2.6E + 07	2.8E + 04	1.3E + 07	12 (2/17)	100 (2/2)

The values from this study (RNA copy/approx. 3 mm³ tissue) were converted to RNA copy/g tissue by assuming the tissue density was approximately that of water (1,000 kg/m³, i.e., 1 g = 1,000 mg, equivalent to a volume of 1,000 mm³).

^aAll 11 study patients were included.

cardio-renal axis [Crackower et al., 2002; Harmer et al., 2002; Vickers et al., 2002]. It has been shown that the distribution of ACE-2 is mainly in the cardio-renal axis and the gastrointestinal system, particularly the ileum, duodenum, jejunum, caecum, and colon. Interestingly, the mRNA coding for ACE-2 has been found in up to 72 human tissues, many of which that do not actually express the enzyme itself [Harmer et al., 2002; Chiu et al., 2004]. The gene coding for ACE-2 is located on the X chromosome (Xp22) [Tipnis et al., 2000], and since the 2003 SARS epidemics, there has been some speculation as to whether allelic variants of ACE-2 may have affected male and female SARS patients differently, though this has not been proven so far [Chiu et al., 2004].

Together, the expression of these two receptors on human body organs and tissues support the tropism for SARS-CoV, as demonstrated in this study and by Farcas et al. [2005]. The identification of the receptors and the tissues in which they are expressed most highly may explain more clearly the pathogenesis and clinical spectrum of SARS.

ACKNOWLEDGMENTS

This project was supported by the Research Fund for the Control of Infectious Diseases (RFCID) from the Health, Welfare and Food Bureau of the Hong Kong Special Administrative Region Government. Part of the work was performed at the Lo Kwee Cheong Research Laboratory.

REFERENCES

- Chan PK, To KF, Lo AW, Cheung JL, Chu I, Au FW, Tong JH, Tam JS, Sung JJ, Ng HK. 2004a. Persistent infection of SARS coronavirus in colonic cells in vitro. *J Med Virol* 74:1–7.
- Chan PK, To WK, Ng KC, Lam RK, Ng TK, Chan RC, Wu A, Yu WC, Lee N, Hui DS, Lai ST, Hon EK, Li CK, Sung JJ, Tam JS. 2004b. Laboratory diagnosis of SARS. *Emerg Infect Dis* 10:825–831.
- Chan WS, Wu C, Chow SC, Cheung T, To KF, Leung WK, Chan PK, Lee KC, Ng HK, Au DM, Lo AW. 2005. Coronaviral hypothetical and structural proteins were found in the intestinal surface enterocytes and pneumocytes of severe acute respiratory syndrome (SARS). *Mod Pathol* 18:1432–1439.
- Chau TN, Lee KC, Yao H, Tsang TY, Chow TC, Yeung YC, Choi KW, Tso YK, Lau T, Lai ST, Lai CL. 2004. SARS-associated viral hepatitis caused by a novel coronavirus: Report of three cases. *Hepatology* 39:302–310.
- Cheng PK, Wong DA, Tong LK, Ip SM, Lo AC, Lau CS, Yeung EY, Lim WW. 2004. Viral shedding patterns of coronavirus in patients with probable severe acute respiratory syndrome. *Lancet* 363:1699–1700.
- Chiu RW, Tang NL, Hui DS, Chung GT, Chim SS, Chan KC, Sung YM, Chan LY, Tong YK, Lee WS, Chan PK, Lo YM. 2004. ACE2 gene polymorphisms do not affect outcome of severe acute respiratory syndrome. *Clin Chem* 50:1683–1686.
- Chow KC, Hsiao CH, Lin TY, Chen CL, Chiou SH. 2004. Detection of severe acute respiratory syndrome-associated coronavirus in pneumocytes of the lung. *Am J Clin Pathol* 121:574–580.
- Crackower MA, Sarao R, Oudit GY, Yagil C, Kozieradzki I, Scanga SE, Oliveira-dos-Santos AJ, da Costa J, Zhang L, Pei Y, Scholey J, Ferrario CM, Manoukian AS, Chappell MC, Backx PH, Yagil Y, Penninger JM. 2002. Angiotensin-converting enzyme 2 is an essential regulator of heart function. *Nature* 417:822–828.
- Ding Y, Wang H, Shen H, Li Z, Geng J, Han H, Cai J, Li X, Kang W, Weng D, Lu Y, Wu D, He L, Yao K. 2003. The clinical pathology of severe acute respiratory syndrome (SARS): A report from China. *J Pathol* 200:282–289.
- Ding Y, He L, Zhang Q, Huang Z, Che X, Hou J, Wang H, Shen H, Qiu L, Li Z, Geng J, Cai J, Han H, Li X, Kang W, Weng D, Liang P, Jiang S. 2004. Organ distribution of severe acute respiratory syndrome (SARS) associated coronavirus (SARS-CoV) in SARS patients: Implications for pathogenesis and virus transmission pathways. *J Pathol* 203:622–630.
- Farcas GA, Poutanen SM, Mazzulli T, Willey BM, Butany J, Asa SL, Faure P, Akhavan P, Low DE, Kain KC. 2005. Fatal severe acute respiratory syndrome is associated with multiorgan involvement by coronavirus. *J Infect Dis* 191:193–197.
- Franks TJ, Chong PY, Chui P, Galvin JR, Lourens RM, Reid AH, Selbs E, McEvoy CP, Hayden CD, Fukuoka J, Taubenberger JK, Travis WD. 2003. Lung pathology of severe acute respiratory syndrome (SARS): A study of 8 autopsy cases from Singapore. *Hum Pathol* 34:743–748.
- Hamming I, Timens W, Bulthuis ML, Lely AT, Navis GJ, van Goor H. 2004. Tissue distribution of ACE2 protein, the functional receptor for SARS coronavirus. A first step in understanding SARS pathogenesis. *J Pathol* 203:631–637.
- Harmer D, Gilbert M, Borman R, Clark KL. 2002. Quantitative mRNA expression profiling of ACE 2, a novel homologue of angiotensin converting enzyme. *FEBS Lett* 532:107–110.
- Hung IF, Cheng VC, Wu AK, Tang BS, Chan KH, Chu CM, Wong MM, Hui WT, Poon LL, Tse DM, Chan KS, Woo PC, Lau SK, Peiris JS, Yuen KY. 2004. Viral loads in clinical specimens and SARS manifestations. *Emerg Infect Dis* 10:1550–1557.
- Jeffers SA, Tusell SM, Gillim-Ross L, Hemmila EM, Achenbach JE, Babcock GJ, Thomas WD, Jr., Thackray LB, Young MD, Mason RJ, Ambrosino DM, Wentworth DE, Demartini JC, Holmes KV. 2004. CD209L (L-SIGN) is a receptor for severe acute respiratory syndrome coronavirus. *Proc Natl Acad Sci USA* 101:15748–15753.
- Lang ZW, Zhang LJ, Zhang SJ, Meng X, Li JQ, Song CZ, Sun L, Zhou YS, Dwyer DE. 2003. A clinicopathological study of three cases of severe acute respiratory syndrome (SARS). *Pathology* 35:526–531.

- Lau YL, Peiris JM. 2005. Pathogenesis of severe acute respiratory syndrome. *Curr Opin Immunol* 17:404–410.
- Lee N, Allen Chan KC, Hui DS, Ng EK, Wu A, Chiu RW, Wong VW, Chan PK, Wong KT, Wong E, Cockram CS, Tam JS, Sung JJ, Lo YM. 2004. Effects of early corticosteroid treatment on plasma SARS-associated Coronavirus RNA concentrations in adult patients. *J Clin Virol* 31:304–309.
- Li W, Moore MJ, Vasilieva N, Sui J, Wong SK, Berne MA, Somasundaran M, Sullivan JL, Luzuriaga K, Greenough TC, Choe H, Farzan M. 2003. Angiotensin-converting enzyme 2 is a functional receptor for the SARS coronavirus. *Nature* 426:450–454.
- Mazzulli T, Farcas GA, Poutanen SM, Willey BM, Low DE, Butany J, Asa SL, Kain KC. 2004. Severe acute respiratory syndrome-associated coronavirus in lung tissue. *Emerg Infect Dis* 10:20–24.
- Nicholls JM, Poon LL, Lee KC, Ng WF, Lai ST, Leung CY, Chu CM, Hui PK, Mak KL, Lim W, Yan KW, Chan KH, Tsang NC, Guan Y, Yuen KY, Peiris JS. 2003. Lung pathology of fatal severe acute respiratory syndrome. *Lancet* 361:1773–1778.
- Peiris JS, Chu CM, Cheng VC, Chan KS, Hung IF, Poon LL, Law KI, Tang BS, Hon TY, Chan CS, Chan KH, Ng JS, Zheng BJ, Ng WL, Lai RW, Guan Y, Yuen KY. HKU/UCH SARS Study Group. 2003. Clinical progression and viral load in a community outbreak of coronavirus-associated SARS pneumonia: A prospective study. *Lancet* 361:1767–1772.
- Shi X, Gong E, Gao D, Zhang B, Zheng J, Gao Z, Zhong Y, Zou W, Wu B, Fang W, Liao S, Wang S, Xie Z, Lu M, Hou L, Zhong H, Shao H, Li N, Liu C, Pei F, Yang J, Wang Y, Han Z, Shi X, Zhang Q, You J, Zhu X, Gu J. 2005. Severe acute respiratory syndrome associated coronavirus is detected in intestinal tissues of fatal cases. *Am J Gastroenterol* 100:169–176.
- Tipnis SR, Hooper NM, Hyde R, Karran E, Christie G, Turner AJ. 2000. A human homolog of angiotensin-converting enzyme. Cloning and functional expression as a captopril-insensitive carboxypeptidase. *J Biol Chem* 275:33238–33243.
- To KF, Lo AW. 2004. Exploring the pathogenesis of severe acute respiratory syndrome (SARS): The tissue distribution of the coronavirus (SARS-CoV) and its putative receptor, angiotensin-converting enzyme 2 (ACE2). *J Pathol* 203:740–743.
- To KF, Tong JH, Chan PK, Au FW, Chim SS, Chan KC, Cheung JL, Liu EY, Tse GM, Lo AW, Lo YM, Ng HK. 2004. Tissue and cellular tropism of the coronavirus associated with severe acute respiratory syndrome: An in-situ hybridization study of fatal cases. *J Pathol* 202:157–163.
- Tse GM, To KF, Chan PK, Lo AW, Ng KC, Wu A, Lee N, Wong HC, Mak SM, Chan KF, Hui DS, Sung JJ, Ng HK. 2004. Pulmonary pathological features in coronavirus associated severe acute respiratory syndrome (SARS). *J Clin Pathol* 57:260–265.
- Vickers C, Hales P, Kaushik V, Dick L, Gavin J, Tang J, Godbout K, Parsons T, Baronas E, Hsieh F, Acton S, Patane M, Nichols A, Tummino P. 2002. Hydrolysis of biological peptides by human angiotensin-converting enzyme-related carboxypeptidase. *J Biol Chem* 277:14838–14843.
- Wang P, Chen J, Zheng A, Nie Y, Shi X, Wang W, Wang G, Luo M, Liu H, Tan L, Song X, Wang Z, Yin X, Qu X, Wang X, Qing T, Ding M, Deng H. 2004. Expression cloning of functional receptor used by SARS coronavirus. *Biochem Biophys Res Commun* 315:439–444.
- Woo PC, Lau SK, Huang Y, Tsoi HW, Chan KH, Yuen KY. 2005. Phylogenetic and recombination analysis of coronavirus HKU1, a novel coronavirus from patients with pneumonia. *Arch Virol* 150:2299–2311.
- Xiao X, Chakraborti S, Dimitrov AS, Gramatikoff K, Dimitrov DS. 2003. The SARS-CoV S glycoprotein: Expression and functional characterization. *Biochem Biophys Res Commun* 312:1159–1164.
- Xu D, Zhang Z, Jin L, Chu F, Mao Y, Wang H, Liu M, Wang M, Zhang L, Gao GF, Wang FS. 2005. Persistent shedding of viable SARS-CoV in urine and stool of SARS patients during the convalescent phase. *Eur J Clin Microbiol Infect Dis* 24:165–171.
- Zhao JM, Zhou GD, Sun YL, Wang SS, Yang JF, Meng EH, Pan D, Li WS, Zhou XS, Wang YD, Lu JY, Li N, Wang DW, Zhou BC, Zhang TH. 2003. Clinical pathology and pathogenesis of severe acute respiratory syndrome. *Zhonghua Shi Yan He Lin Chuang Bing Du Xue Za Zhi* 17:217–221.